



Performance improvement of phenyl acetate as propylene carbonate-based electrolyte additive for lithium ion battery by fluorine-substituting

Bin Li ^a, Yaqiong Wang ^b, Haibin Lin ^b, Xianshu Wang ^b, Mengqing Xu ^b, Yating Wang ^b, Lidan Xing ^b, Weishan Li ^{a, b, *}

^a College of Materials Science and Engineering, South China University of Technology, Guangzhou 510641, China

^b School of Chemistry and Environment, Key Laboratory of Electrochemical Technology on Energy Storage and Power Generation of Guangdong Higher Education Institutes, Engineering Research Center of Materials and Technology for Electrochemical Energy Storage, Ministry of Education, South China Normal University, Guangzhou 510006, China

H I G H L I G H T S

- Performance of PA as electrolyte additive of Li-ion battery is improved by F-substituting.
- 4-FPA is more effective than PA for forming SEI on graphite in PC-based electrolyte.
- 4-FPA improves cyclic stability of Li-ion battery using PC-based electrolyte.
- Incorporation of 4-FPA reduction products into SEI contributes to the improved performance.

A R T I C L E I N F O

Article history:

Received 13 February 2014

Received in revised form

22 April 2014

Accepted 7 May 2014

Available online 21 May 2014

Keywords:

Lithium ion battery

Propylene carbonate-based electrolyte

4-Fluorophenyl acetate

Solid electrolyte interphase

Graphite

A B S T R A C T

Phenyl acetate (PA) is more stable and much cheaper than vinylene carbonate (VC), a commercial electrolyte additive for graphite anode of lithium ion battery, but its performance needs to be improved. In this paper, we report a new additive, 4-fluorophenyl acetate (4-FPA), which results from the fluorine-substituting of PA. The properties of the formed solid electrolyte interphase (SEI) by 4-FPA are investigated comparatively with PA by molecular energy level calculation, cyclic voltammetry, charge–discharge test, scanning electron microscopy, energy dispersive X-ray spectroscopy, and Fourier transform infrared spectroscopy. It is found that the SEI formed by 4-FPA is more protective than PA, resulting in the improved cyclic stability of lithium ion battery: the capacity retention of LiFePO₄/graphite cell after 90 cycles is 92% for 4-FPA but only 84% for PA. The fluorine in 4-FPA makes it more reducible than PA and the fluorine-containing reduction products of 4-FPA are incorporated into the SEI, which contributes to the improved performance.

© 2014 Elsevier B.V. All rights reserved.

1. Introduction

Lithium ion battery is regarded as a promising power source for electric vehicles because of its high energy density and long cycle life compared to other secondary batteries [1,2]. The electrolyte is a key component in battery. The electrolyte used in currently commercial lithium ion battery is LiPF₆ dissolved in the mixture of linear and cyclic carbonates. Compared to the varied linear

carbonates, only ethylene carbonate (EC) and propylene carbonate (PC) are available as cyclic carbonates. EC has a poor low-temperature performance due to its high melting point, while PC is in liquid over a wide range of temperature and has a high dielectric constant [3]. However, PC decomposes easily on graphite anode and co-intercalates into graphite with lithium ion, which causes the volume expansion and exfoliation of graphite and thus leads to the capacity loss and cycling instability of battery [4,5].

To prevent PC co-intercalation, electrolyte additives for forming solid electrolyte interphase (SEI) on graphite should be used. The ideal SEI allows the intercalation/de-intercalation of lithium ion but prevents the solvent molecule and anion intercalation into the graphite anode [6–8]. Many additives are found to be effective for

* Corresponding author. School of Chemistry and Environment, South China Normal University, Guangzhou 510006, China. Tel./fax: +86 20 39310256.

E-mail address: liwsh@scnu.edu.cn (W. Li).

the SEI formation, such as vinylene carbonate (VC) [9], propylene sulfite [10], propane sultone [11], prop-1-ene-1, 3-sultone [12,13], 2-phenylimidazole [14], 4,5-dimethyl-(1,3)dioxol-2-one [15], phenyl tris-2-methoxydiethoxy silane [16], and boron-based compounds [17,18]. The successful applications of these additives are based on their preferable reduction to solvents. Among these additives, VC is the most effective for the formation of a stable SEI and has been widely used in commercial lithium ion battery. However, VC is known as an unstable compound due to the vinyl group and tends to polymerize on cathode of lithium ion battery [9,19]. Furthermore, VC is very expensive.

Aromatic ester such as phenyl acetate (PA) was also used as an additive of PC-based electrolyte [20,21]. The well-conjugated structure in PA makes it more stable than VC but more reducible than solvents, which facilitates the formation of a protective SEI. Most importantly, PA is cheap and its price is only one fiftieth of VC. However, PA behaves poorer than VC as an SEI forming additive.

Fluorine-containing electrolyte additives have been developed to form a stable SEI [22–24]. Fluorine is an electrondrawing group, which makes the additives more electrophilic and reducible. Introduction of fluorine into organic molecules usually reduces their boiling temperature and viscosity that may affect the low-temperature performance of the battery [25].

The purpose of this work is to improve the performance of PA as SEI-forming additive in PC-based electrolyte by fluorine-substituting. 4-Fluorophenyl acetate (4-FPA) was selected in this work, because it has highest reduction activity among all the single fluorine substituted PAs. The properties of the formed SEI by 4-FPA were investigated comparatively with PA by using molecular energy level calculation, cyclic voltammetry, charge–discharge test, scanning electron microscopy, energy dispersive X-ray spectroscopy, and Fourier transform infrared spectroscopy.

2. Experimental

The energy levels of the lowest unoccupied molecule orbital (LUMO) of organic molecules were calculated by the Gaussian 03 program package [26]. The equilibrium state structure is optimized by B3LYP method at 6-311+G (d) basis set, in gas phase. The frontier orbital energy is analyzed by the natural bond orbital (NBO) theory.

The battery grade solvents, PC and ethyl methyl carbonate (EMC), were provided by Guangzhou Tinci Materials Technology Co. Ltd., China. Lithium hexafluorophosphate (LiPF_6 , battery grade) was purchased from Hashimoto Chemical Corporation. 4-FPA (99.4%) was purchased from Fujian Chuangxin Science and Technology Develops Co. Ltd, Fuzhou, China, and PA (>99%) from Aladdin. All these chemicals were used without further purification. The base electrolyte used in this work is 1 mol dm^{-3} LiPF_6 in PC/EMC (1/3, in weight). The electrolyte was prepared in a glove box (Mbraun Unilab MB20) under a dry argon atmosphere (the content of water and oxygen was controlled to lower than 0.1 ppm).

2025-type coin cells of Li/graphite and LiFePO_4 /graphite were assembled in the glove box (Mbraun Unilab MB20) for cyclic voltammetry and charge–discharge tests. The graphite electrode was prepared by mixing 89 wt % natural graphite (Shanshan Tech Co., Ltd, China), 4 wt % Ks6 (Timrex), 2 wt % super-p (MMM carbon, Belgium), and 5 wt % poly (vinylidene difluoride) (PVdF, Ofluorine Chemical Tech Co., Ltd, China) binder in N-methyl-2-pyrrolidone, coating and pressing the mixture onto a copper foil current collector. The LiFePO_4 electrode was prepared by coating a mixture of 90 wt% LiFePO_4 (Tianjin Stl Energy Technology Co., Ltd), 5 wt% super-p, and 5 wt% poly (vinylidene difluoride) (PVdF) binder onto an aluminum foil current collector. Celgard 2300 microporous membrane was used as the separator. The capacity reported in this

paper is based on the weight of the mixture rather than the active material. Each coin cell contained 30 μL of electrolyte.

The charge–discharge tests were conducted on a LAND cell test system (Land CT 2001A). The Li/graphite cells were charged and discharged in the potential range of 0.01–2.5 V (vs. Li^+/Li) at 0.1C rate, while the LiFePO_4 /graphite cells were cycled between 2.0 and 3.85 V at 0.3C rate. Cyclic voltammetry was performed on Solartron-1480 (England) in the potential range of 0.01–2.5 V (vs. Li^+/Li) at a scanning rate of 0.1 mV s^{-1} . Five cells were tested with each electrolyte and the reported charge–discharge results are the average values of top three cells in terms of discharge capacity.

The graphite electrodes for structure and composition characterizations were rinsed three times with dimethyl carbonate in the glove box (Mbraun Unilab MB20) to remove LiPF_6 salt precipitated on the electrodes, and then evacuated overnight in the transfer chamber of the glove box. Scanning electron microscopy (SEM) and energy dispersive X-ray spectroscopy (EDS) analyses were conducted on a JEOL-5900 SEM. The Fourier transform infrared spectroscopy (FTIR) measurement was carried out on a BRUKER TENSOR27 spectrophotometer within $400\text{--}4000 \text{ cm}^{-1}$ using a transmittance mode. The samples for the SEM, EDS and FTIR measurements were transferred in a hermetical sealed glass vial to avoid the exposure to air.

3. Results and discussion

3.1. LUMO energy

Theoretical calculations were performed to compare the electrochemical reduction ability of additives and solvents. It is known that the lowest unoccupied molecular orbital (LUMO) energy corresponds to the reduction decomposition potential of organic molecules. The lower the LUMO level of a molecule is, the more easily the electron can be transferred into the molecule. An ideal SEI-forming additive should have a lower LUMO energy than the electrolyte solvents. The calculated LUMO energies of EMC, PC, PA, 2-fluorophenyl acetate, 3-fluorophenyl acetate, 4-fluorophenyl acetate (4-FPA) are given in Table 1. It can be seen from Table 1 that the LUMO energies are in the order of $\text{EMC} > \text{PC} > \text{PA} > 2\text{-fluorophenyl acetate} > 3\text{-fluorophenyl acetate} > 4\text{-FPA}$. PC has a lower LUMO energy than EMC, showing its disservice to battery performance due to its preferable reduction and subsequent co-intercalation into graphite. The lower LUMO energy of PA than that of PC confirms that PA can be used as an electrolyte additive for SEI formation on anode of lithium ion battery. It can be noted that three fluorophenyl acetates have lower LUMO energies than PA, showing that the fluorine-substituting improves the reducibility of PA. The LUMO energy of 4-FPA is lowest among three fluorophenyl acetates, indicating that 4-FPA is most reducible. Therefore, 4-FPA is selected in this work and it is expected that the co-intercalation of PC into graphite would be suppressed more effectively by 4-FPA than PA.

3.2. Effect of 4-FPA on co-intercalation of PC

Cyclic voltammetry was performed to understand the effect of the additives on the co-intercalation of PC into graphite. Fig. 1 shows the cyclic voltammograms of graphite electrodes in 1 mol dm^{-3} LiPF_6 /PC-EMC (1:3) base and additive-containing electrolytes. From the voltammogram of the electrode in the base electrolyte at the first cycle (Fig. 1(a)), it can be seen that the initial electrolyte reduction current appears at about 0.75 V (vs. Li^+/Li), followed by a current peak at about 0.35 V (vs. Li^+/Li) and the increased current from about 0.25 V (vs. Li^+/Li). The initial reduction current should be mainly ascribed to the decomposition and co-intercalation of PC. The current peak indicates that the electron

Table 1
LUMO energies of EMC, PC, PA, and FPAs.

Organic molecules	LUMO energy (eV)
Ethyl methyl carbonate	0.0735
Propylene carbonate	−0.3045
Phenyl acetate	−0.9731
2-Fluorophenyl acetate	−1.2101
3-Fluorophenyl acetate	−1.2324
4-Fluorophenyl acetate (4-FPA)	−1.3159

transfer for the PC reduction is so fast that the reaction is controlled by diffusion. The increased current results mainly from the lithium intercalation into graphite, which can be confirmed by the oxidation current peaks at about 0.3 V (vs. Li^+/Li) during backward scan. It should be noted that the current peak for the PC decomposition can be still observed when the electrode is cycled further (at the 2nd and 3rd cycles), suggesting that the SEI formed on the graphite in the base electrolyte cannot prevent the decomposition and co-intercalation of PC. This is why additives should be used in the lithium ion battery using PC-based electrolyte.

Different voltammetric behaviors of the electrode were recorded in the electrolytes with additives, as shown in Fig. 1(b) and (c). Fig. 1(d) presents a comparison of the voltammograms of the electrode in the base and additive-containing electrolytes at the first cycle. It can be seen from Fig. 1(d) that the initial decomposition of the additive-containing electrolytes takes place earlier than that of the base electrolyte, from 0.75 V to 1.0 V (vs. Li^+/Li), indicative of the preferable reduction of PA or 4-FPA to the solvents. For the electrolyte containing PA (Fig. 1(b)), the current peak for decomposition and co-intercalation of PC disappears at the 3rd cycle but can still be observed at the 2nd cycle. This result shows that the preferable reduction of PA can inhibit the decomposition and co-intercalation of PC to some extent but not effective. The inhibition of PC decomposition and co-intercalation should be ascribed to the formation of a protective SEI.

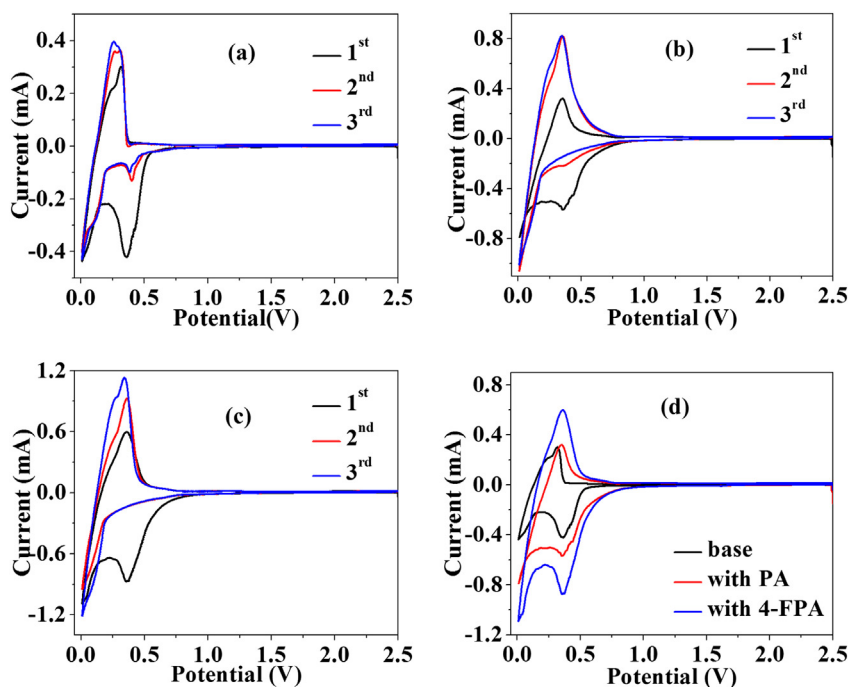


Fig. 1. Voltammograms of graphite electrode in 1 mol dm^{-3} $\text{LiPF}_6/\text{PC-EMC}$ (1:3) without additive (a), with 4 wt% PA (b) and 4 wt% 4-FPA (c); a comparison of the first cycle voltammogram (d). Scan rate: 0.1 mV s^{-1} .

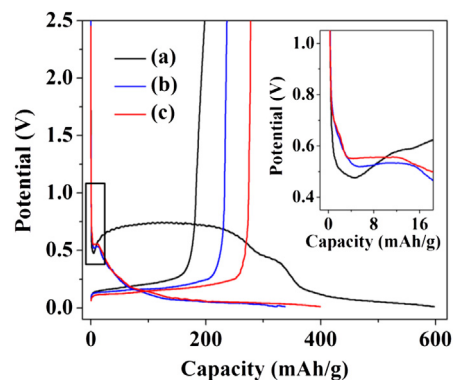


Fig. 2. Charge–discharge characteristics of Li/graphite cells using 1 mol dm^{-3} $\text{LiPF}_6/\text{PC-EMC}$ (1:3) without additive (a), with 4 wt% PA (b) and 4 wt% 4-FPA (c).

For the electrolyte containing 4-FPA (Fig. 1(c)), the current peak for decomposition and co-intercalation of PC disappears from the 2nd cycle, suggesting that a more protective SEI can be formed by 4-FPA than PA. The potential for the initial reduction of 4-FPA is almost the same as that of PA, but the subsequent current on the electrode in the 4-FPA-containing electrolyte is larger than that in the PA-containing electrolyte, confirming that 4-FPA is reduced more easily than PA. Since the initial potentials are the same for both additives, the better inhibition of PC-intercalation by fluorine-containing 4-FPA than fluorine-free PA should be related to the improved stability of SEI due to the incorporation of the fluorine-containing reduction products of 4-FPA. As an SEI-forming additive, its preferable reduction to solvents is important, but its structure cannot be neglected because its reduction products might be incorporated into the resulting SEI.

Charge–discharge test by constant current confirms the inhibition of PC co-intercalation by the additives. Fig. 2 presents the first charge–discharge curves of Li/graphite cells in 1 mol dm^{-3}

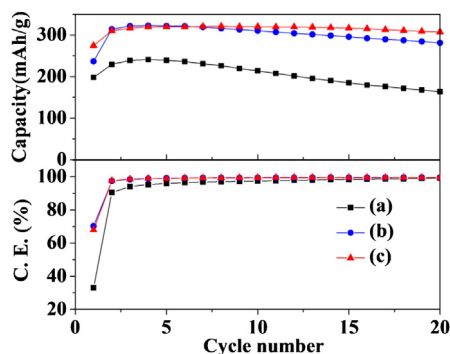


Fig. 3. Cycling performances of Li/graphite cells in 1 mol dm⁻³ LiPF₆/PC-EMC (1:3) without additive (a), with 4 wt% PA (b) and 4 wt% 4-FPA (c).

LiPF₆/PC-EMC (1:3) electrolyte with and without additives. For the base electrolyte, the potential of the charged graphite electrode drops quickly to about 0.47 V (vs. Li⁺/Li), then rises to about 0.72 V (vs. Li⁺/Li) and remains unchanged for a long time. This performance results from the co-intercalation of PC with lithium ions into graphite, which causes a large irreversible capacity loss. The discharge capacity of the cell in the first cycle is 198 mAh g⁻¹ with a coulombic efficiency of 33.1%. For the cell with PA, a slowly decreasing potential starting from about 0.7 V (vs. Li⁺/Li) and a short potential plateau at 0.52 V (vs. Li⁺/Li) are observed, as shown in the inset of Fig. 2. The short potential plateau can be ascribed to the reduction of PA, responsible for the formation of SEI film on graphite electrode. The SEI film formed by PA inhibits the co-intercalation of PC into graphite, leading to the improved performance of the cell. The discharge capacity of the cell in the first cycle is 237 mAh g⁻¹ with a coulombic efficiency of 70.3%. In the electrolyte with 4-FPA, similar behavior to the electrolyte with PA is observed. It should be noted that the potential plateau for the SEI formation is higher than that of PA, indicating that the 4-FPA has higher reduction activity than PA. As a result, cell performance is improved further by the addition of 4-FPA. The discharge capacity of the cell with 4-FPA in the first cycle is 276 mAh g⁻¹ with a coulombic efficiency of 68.0%. The lower initial coulombic efficiency of the cell using 4-FPA than that using PA suggests that more 4-FPA is reduced than PA during the SEI formation.

Fig. 3 presents the cycling performances of the Li/graphite cells in 1 mol dm⁻³ LiPF₆/PC-EMC (1:3) electrolyte with and without

Table 2

Element contents of the fresh and cycled graphite electrodes in 1 mol dm⁻³ LiPF₆/PC-EMC (1:3) without and with additives.

Electrolyte	C (At. %)	O (At. %)	F (At. %)
Fresh	92.37	2.61	5.02
Base Electrolyte	58.97	33.82	7.21
With PA	70.80	22.82	6.38
With 4-FPA	85.49	8.48	6.03

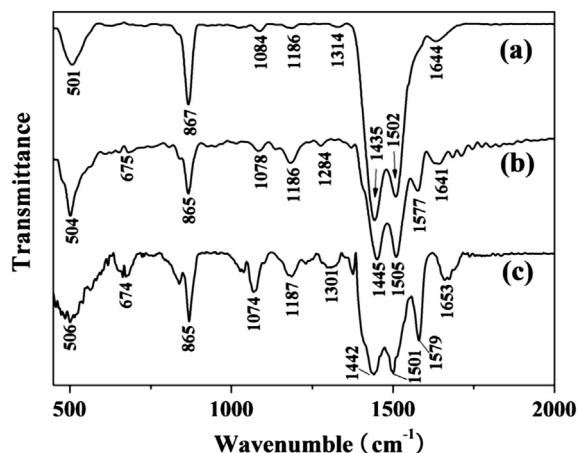


Fig. 5. FTIR spectra of graphite after the first cycle in 1 mol dm⁻³ LiPF₆/PC-EMC (1:3) without additive (a), with 4 wt% PA (b) and with 4 wt% 4-FPA (c).

additives. It can be seen from the curve a of Fig. 3 that the cell without additive experiences a serious capacity fading during cycling. This indicates that no protective SEI is formed on graphite in PC-based electrolyte without any additive and the co-intercalation of PC leads to the exfoliation of the graphite. In the presence of PA, the reversible capacity of the cell is improved. However, the capacity fading can still be observed during cycling, as shown in the curve b of Fig. 3. The discharge capacity of the cell using PA-containing electrolyte becomes 281 mAh g⁻¹ after 20 cycles. This result confirms that the SEI formed by PA can inhibit the decomposition and co-intercalation of PC but the inhibition is not effective. As shown in the curve c of Fig. 3, 4-FPA substantially improves the cyclic performance of the cell. With using the electrolyte containing 4-FPA, the discharge capacity of the cell maintains 308 mAh g⁻¹ after 20 cycles

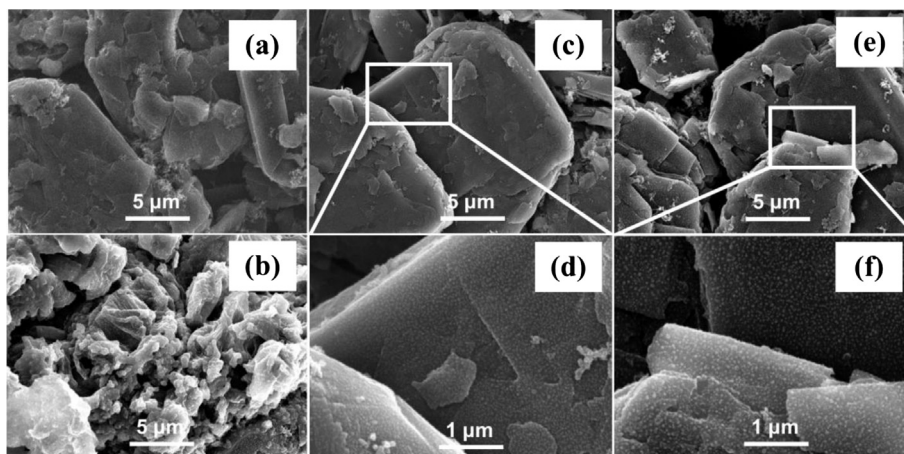
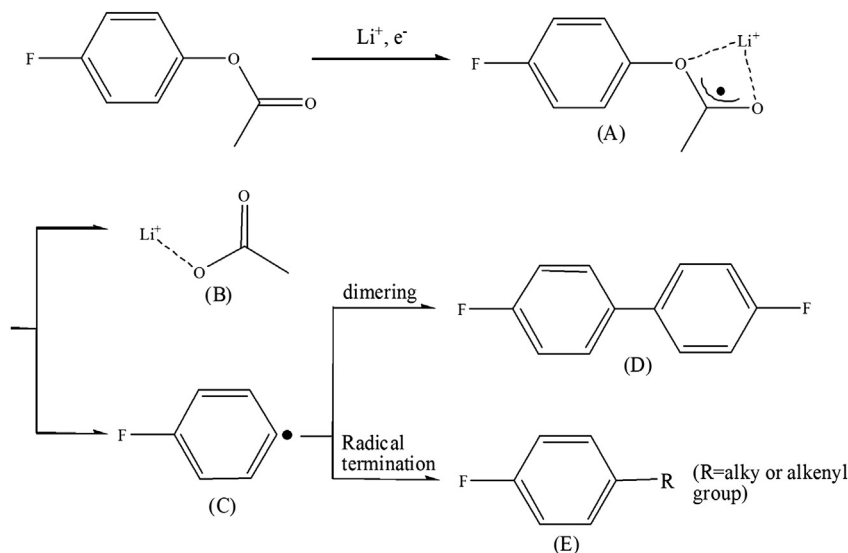


Fig. 4. SEM images of graphite electrodes: before cycling (a), after the first cycle in 1 mol dm⁻³ LiPF₆/PC-EMC (1:3) without additive (b), with 4 wt% PA (c, d) and with 4 wt% 4-FPA (e, f).



Scheme 1. Possible reaction paths for the reduction of 4-FPA on graphite electrode.

with a coulombic efficiency of 99.6%. It is obvious that the fluorine-substituting improves the effectiveness of PA for forming a protective SEI on graphite in PC-based electrolyte.

3.3. Surface morphology and composition of graphite

To confirm the incorporation of the reduction products of 4-FPA into the SEI, the surface morphology and composition of the cycled graphite electrode were characterized with SEM, EDS and FTIR.

Fig. 4 presents the SEM images of the graphite electrodes before and after the first cycle. Before cycling, the grain graphite particles with clean surface can be identified, as shown in Fig. 4(a). When the graphite electrode was cycled in the base electrolyte, the graphite particles were broken and turned to be flake-like, as shown in Fig. 4(b). It is obvious that the graphite suffers exfoliation due to the co-intercalation of PC. However, this situation did not happen when the graphite electrode was cycled in the PA or 4-FPA-containing electrolyte. It can be seen from Fig. 4(c) and (e) that the shape of the graphite particles remains unchanged and a layer of deposit was formed on the graphite, indicating that a protective SEI film has been formed due to the use of PA or 4-FPA. There is no significant difference in morphology of the graphite between the electrodes cycled in the PA and 4-FPA-containing electrolytes.

The element contents of the fresh and cycled graphite electrodes, estimated from EDS, are shown in Table 2. It can be seen

from Table 2 that three electrodes are composed of the same elements, C, O and F, which mainly result from the electrolyte decompositions including solvents and salt, but the contents are different. The concentration of C is decreased for both cycled anodes while the concentrations of O, and F are increased compared to the fresh anode electrode, suggesting that the active material is covered by a SEI film. It can be noted from Table 2 that the electrode cycled in the base electrolyte has the largest contents of O and F, suggesting that electrolyte is easy to decompose and confirming that PA or 4-FPA help to build a protective SEI to inhibit electrolyte decomposition. The lower oxygen content in the electrode cycled in 4-FPA-containing electrolyte than that in PA-containing electrolyte confirms that the SEI formed by 4-FPA is more protective than that formed by PA. The largest carbon content in the electrode cycled in 4-FPA-containing electrolyte suggests that the SEI is thin so that more graphite under the SEI can be detected.

Fig. 5 presents the FTIR spectra of graphite electrodes after the first cycle in base and additive-containing electrolytes. Both electrodes have similar FTIR spectra, including the peaks around $1074\text{--}1084\text{ cm}^{-1}$ ($\nu_{\text{C-O}}$), $\sim 1300\text{ cm}^{-1}$ ($\gamma_{\text{SC=O}}$), and $1641\text{--}1653\text{ cm}^{-1}$ ($\nu_{\text{C=O}}$), corresponding to ROCO_2Li , the peaks around $865\text{--}867\text{ cm}^{-1}$ ($\delta_{\text{CO}_3^{2-}}$) and $1435\text{--}1505\text{ cm}^{-1}$ ($\nu_{\text{CO}_3^{2-}}$), corresponding to Li_2CO_3 , and the peaks around $501\text{--}506\text{ cm}^{-1}$, corresponding to the Li–O in ROLi [27–30]. The peak at around 1187 cm^{-1} can be assigned to the C–F stretching which is corresponding to the binder (PVdF) [31]. The signal of C–F at around $1186\text{--}1187\text{ cm}^{-1}$ for the electrode cycled in the base electrolyte (curve a of Fig. 5) is weaker because the peaks of Li_2CO_3 ($1435\text{--}1505\text{ cm}^{-1}$) are too intensive. This result suggests that solvents decompositions happen and the decomposition products deposit on the graphite surface when the cells were cycled in the base or additive-containing electrolyte. However, typical peaks at 674 cm^{-1} and 1579 cm^{-1} appear on the cycled graphite in the additive-containing electrolytes, but cannot be observed on the cycled graphite in the base electrolyte. These peaks are corresponding to aromatic ring [32]. Apparently, the reduction products of PA or 4-FPA are incorporated into the SEI. The SEI is formed in the electrolyte whether it contains additive or not, but 4-FPA or PA is needed to build a protective SEI. It should be noted that the peak intensities of the aromatic ring for the cycled graphite in 4-FPA-containing electrolyte are stronger than those in PA-containing electrolyte, confirming that more reduction products of 4-FPA are incorporated into the SEI than those of PA, which can be attributed

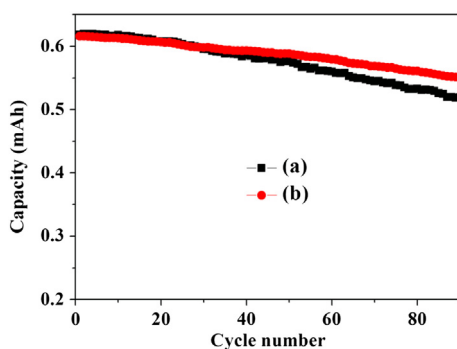


Fig. 6. Cycling performances of the $\text{LiFePO}_4/\text{graphite}$ full coin cells in 1.0 mol dm^{-3} LiPF_6 in PC-EMC (1:3) electrolyte with (a) 4 wt% PA and with 4 wt% 4-FPA (b) at 0.3C current rate.

to preferable reduction of 4-FPA to PA. Since the structure of aromatic ring is more stable than that of the alkyl chains resulting from the decomposition of solvent carbonates, the incorporation of aromatic ring in PA or 4-FPA into SEI improves the stability of SEI for thermal decomposition and electrochemical reduction. Fluorine not only makes the additive more reducible but also improves the stability of SEI. The fluorine in 4-FPA is incorporated into the SEI together with aromatic ring, as shown in Scheme 1, contributing to the improved stability of SEI formed by 4-FPA compared to PA. 4-FPA is reduced on anode forming a radical anion coordinated with lithium ion (A), which might decompose to lithium acetate (B) and radical (C). The radical dimerizes forming dimer (D) or is terminated by other intermediates/solvents to form polymer (E). The resulting dimer and polymer are responsible for the SEI formation and contributes to the performance improvement of PA.

3.4. Battery performance

To evaluate the effect of 4-FPA on battery performance, $\text{LiFePO}_4/\text{graphite}$ coin cells were set up and tested with charge–discharge cycling. Fig. 6 shows cyclic performances of $\text{LiFePO}_4/\text{graphite}$ full coin cells in 1 mol dm^{-3} LiPF_6 in PC-EMC (1:3) electrolytes with PA and 4-FPA. It can be seen from Fig. 6 that the cell using 4-FPA behaves better than the cell using PA. The discharge capacity decreases from 0.62 mAh at the first cycle to 0.52 mAh at the 90th cycle with a capacity retention is 84% for the cell using PA, while from 0.61 mAh to 0.56 mAh with a capacity retention of 92% for the cell using 4-FPA. This result confirms that the SEI formed by 4-FPA is more protective than that formed by PA and can be used as an effective electrolyte additive for lithium ion battery using PC-based electrolyte.

4. Conclusions

The performance of phenyl acetate (PA) as electrolyte additive for lithium ion battery using propylene carbonate-based electrolyte can be improved by fluorine-substituting. This paper presented the effect of a single fluorine substitute of PA, 4-fluorophenyl acetate (4-FPA). It have been demonstrated that 4-FPA is more effective than PA for forming a protective solid electrolyte interphase (SEI) on graphite anode in propylene carbonate-based electrolyte. Due to the fluorine-substituting, 4-FPA exhibits preferable reducibility to PA and helps to build a more protective SEI for graphite to prevent the co-intercalation of propylene carbonate and the exfoliation of graphite, resulting in the improved cyclic stability of lithium ion battery. The incorporation of fluorine and aromatic ring in 4-FPA reduction products into the SEI contributes to the improved protection of SEI for graphite.

Acknowledgment

The authors are highly grateful for the financial support from the joint project of National Natural Science Foundation of China and

Natural Science Foundation of Guangdong Province (Grant No. U1134002), National Natural Science Foundation of China (No. 21003054 and No. 21273084), Natural Science Foundation of Guangdong Province (Grant No. 10351063101000001), key project of Science and Technology in Guangdong Province (Grant No. 2011A010801001), and the scientific research project of DEGP (Grant No. 2013CXZDA013).

References

- [1] J.M. Tarascon, M. Armand, *Nature* 414 (2001) 359–367.
- [2] M. Armand, J.M. Tarascon, *Nature* 457 (2008) 652–657.
- [3] K. Xu, *Chem. Rev.* 104 (2004) 4304–4417.
- [4] M.Q. Xu, W.S. Li, X.X. Zuo, J.S. Liu, X. Xu, *J. Power Sources* 174 (2007) 705–710.
- [5] B. Wang, Q.T. Qu, Q. Xia, Y.P. Wu, X. Li, C.L. Gan, T. van Ree, *Electrochim. Acta* 54 (2008) 816–820.
- [6] M.-S. Zheng, Q.-F. Dong, H.-Q. Cai, M.-G. Jin, Z.-G. Lin, S.-G. Sun, *J. Electrochem. Soc.* 152 (2005) A2207–A2210.
- [7] K. Xu, A.V. Cresce, J. Mater. Chem. 21 (2011) 9849–9864.
- [8] M. Nie, D. Chalasani, D.P. Abraham, Y. Chen, A. Bose, B.L. Lucht, *J. Phys. Chem. C* 117 (2013) 1257–1267.
- [9] D. Aurbach, K. Gamolsky, B. Markovsky, Y. Gofer, M. Schmidt, U. Heider, *Electrochim. Acta* 47 (2002) 1423–1439.
- [10] G.H. Wroldnigg, T.M. Wroldnigg, J.O. Besenhard, M. Winter, *Electrochem. Commun.* 1 (1999) 148–150.
- [11] M.Q. Xu, W.S. Li, B.L. Lucht, *J. Power Sources* 193 (2009) 804–809.
- [12] B. Li, M.Q. Xu, T.T. Li, W.S. Li, S.J. Hu, *Electrochem. Commun.* 17 (2012) 92–95.
- [13] B. Li, M. Xu, B. Li, Y. Liu, L. Yang, W. Li, S. Hu, *Electrochim. Acta* 105 (2013) 1–6.
- [14] B. Wang, Q.T. Qu, L.C. Yang, Q. Xia, Y.P. Wu, D.L. Zhou, X.J. Gu, T. van Ree, *J. Power Sources* 189 (2009) 757–760.
- [15] M. Xu, L. Zhou, L. Xing, W. Li, B.L. Lucht, *Electrochim. Acta* 55 (2010) 6743–6748.
- [16] Q. Xia, B. Wang, Y.P. Wu, H.J. Luo, S.Y. Zhao, T. van Ree, *J. Power Sources* 180 (2008) 602–606.
- [17] K. Xu, U. Lee, S. Zhang, M. Wood, T.R. Jow, *Electrochem. Solid State Lett.* 6 (2003) A144–A148.
- [18] A. Xiao, L. Yang, B.L. Lucht, S.-H. Kang, D.P. Abraham, *J. Electrochem. Soc.* 156 (2009) A318–A327.
- [19] Y. Hu, W. Kong, H. Li, X. Huang, L. Chen, *Electrochem. Commun.* 6 (2004) 126–131.
- [20] J.-T. Lee, M.-S. Wu, F.-M. Wang, Y.-W. Lin, M.-Y. Bai, P.-C.J. Chiang, *J. Electrochem. Soc.* 152 (2005) A1837–A1843.
- [21] P. Ghimire, H. Nakamura, M. Yoshio, H. Yoshitake, K. Abe, *Chem. Lett.* 34 (2005) 1052–1053.
- [22] N. Choi, K.H. Yew, K.Y. Lee, M. Sung, H. Kim, S. Kim, *J. Power Sources* 161 (2006) 1254–1259.
- [23] M.-H. Ryou, G.-B. Han, Y.M. Lee, J.-N. Lee, D.J. Lee, Y.O. Yoon, J.-K. Park, *Electrochim. Acta* 55 (2010) 2073–2077.
- [24] E. Krämer, R. Schmitz, P. Niehoff, S. Passerini, M. Winter, *Electrochim. Acta* 81 (2012) 161–165.
- [25] K. Xu, S.S. Zhang, J.L. Allen, T.R. Jow, *J. Electrochem. Soc.* 149 (2002) A1079–A1082.
- [26] L.D. Xing, C.Y. Wang, W.S. Li, M.Q. Xu, X.L. Meng, S.F. Zhao, *J. Phys. Chem. B* 113 (2009) 5181–5187.
- [27] D. Aurbach, B. Markovsky, A. Schechter, Y. Ein-Eli, *J. Electrochem. Soc.* 143 (1996) 3809–3820.
- [28] Y. Ein-Eli, S.F. McDevitt, B. Markovsky, A. Schechter, D. Aurbach, *J. Electrochem. Soc.* 144 (1997) L180–L184.
- [29] D. Aurbach, B. Markovsky, I. Weissman, E. Levi, Y. Ein-Eli, *Electrochim. Acta* 45 (1999) 67–86.
- [30] L.S. Wang, Y.D. Huang, D.Z. Jia, *Electrochim. Acta* 51 (2006) 4950–4955.
- [31] B. Wang, H.P. Zhang, L.C. Yang, Q.T. Qu, Y.P. Wu, C.L. Gan, D.L. Zhou, *Electrochem. Commun.* 10 (2008) 1571–1574.
- [32] E. Pretch, P. Bühlmann, M. Badertscher (Eds.), *Structure Determination of Organic Compounds: Tables of Spectral Data*, Springer, 2000, p. 280.